Geomech. Geophys. Geo-energ. Geo-resour. (2021)7:107
https://doi.org/10.1007/s40948-021-00296-9

ORIGINAL ARTICLE

Experimental and analytical investigation on the normal contact behavior of natural proppant simulants

Chitta Sai Sandeep · Siyue Li · Kostas Senetakis

Received: 15 January 2021 / Accepted: 2 October 2021

Abstract Granular materials are of interest in various fields of engineering and science and they commonly display rough morphologies which govern their constitutive behavior. One of the emerging applications of granular materials is their use as proppants in hydraulic fracturing and the present study provides an investigation into the normal contact behavior of three types of proppant simulants using micromechanical-based experiments. As the complex processes in hydraulic fracturing necessitate accurate modeling of the order of nano-to-micrometers of displacements, a micromechanical investigation of grain contact response accounting for extremely small ranges of deformations is necessary to provide insights with potential applications in contact mechanics modeling. The proppant simulants used in the present study are composed of quartz sand grains from different origins with variations of their local surface morphologies and nano-to-micro scale roughness. Based on their local radii, which govern the contact behavior of non-conforming surfaces, the proppant simulants would approximately correspond to mesh 16/30–20/40. In view of their global radii, these grains would be considered on the upper bound of potential sizes used in hydraulic fracturing. In terms of normal contact response, the data were fitted using two contact mechanics models and a discussion is elaborated on their applicability in simulating the normal load–displacement behavior of grains at their contacts. It is shown that surface asperities play an important role in the constitutive behavior of the grain contacts and control the different zones of response as observed from both experiments and analytical expressions. Natural grains used as proppants may display smoother surfaces compared with other geological materials, such as weathered rocks or crushed rocks. However, their roughness is still an important influencing factor that should be considered in the simulation of multi-scale problems, especially when micrometer-level displacements are important to be encountered. Based on differentiation of the normal force for a given range of displacements, tangent stiffness was derived and the data showed that tangent normal stiffness (K_N) increases with normal displacement. Thus, the load (or stress) state of a given contact is important to provide appropriate values of the ratio (K_T/K_N), where the tangential stiffness (K_T) decreases rapidly with the increase of the sliding displacement.

C. S. Sandeep
School of Civil and Construction Engineering, Oregon State University, Corvallis, Oregon 97331, USA
e-mail: chittas@oregonstate.edu

S. Li · K. Senetakis (✉)
Department of Architecture and Civil Engineering, City University of Hong Kong, Yeung Kin Man Academic Building, Blue Zone 6/F, Kowloon, Hong Kong SAR, China
e-mail: ksenetak@cityu.edu.hk

S. Li
e-mail: siyueli6-c@my.cityu.edu.hk

Published online: 02 November 2021

Article highlights

- Three types of natural proppant simulants are examined using micromechanical-based experiments exploring their normal contact behavior.
- Surface roughness controls normal contact stiffness and initial plastic deformations at the contacts.
- Different approaches should be adopted on the implementation of input parameters using smooth or rough surface contact models in discrete-based numerical analyses.

Keywords Proppant · Normal contact stiffness · Roughness · Morphology · Micromechanics

1 Introduction

Horizontal drilling and multi-stage hydraulic fracturing are required in unconventional reservoir exploitation; these involve multi-scale and multi-phase complex processes and encounter a large number of influencing factors (Bandara et al. 2018, De Silva and Ranjith 2019a, b, Zoback and Kohli 2019, Duan and Kwok 2020, Kwok and Duan 2020, Ahamed et al. 2019). In hydraulic fracturing, different types of proppants are commonly used, including natural sand grains, so that the interactions of proppants at their contacts and between proppants and the rock is crucial to be modeled and understood (Bandara et al. 2020a, Dong et al. 2019, Tang et al. 2019, Zheng and Tannant 2019, Wang and Sharma 2018, Wang et al. 2019). Researchers have applied experimental grain-scale methods to investigate the problem of proppant-proppant and proppant-rock interactions (Yang et al. 2016, Zhang et al. 2019a, b, Ahamed et al. 2019, Bandara et al. 2018, 2020a, b, Tang et al. 2019, Li et al. 2021). He and Senetakis (2020) and He et al. (2020) reported that both proppant, rock type and their morphological features, including surface roughness at a microscopic scale of tens-to-hundreds of nanometers, influence their tribological behavior. Bandara et al. (2020a), stated that current methods and guidelines may be, partly, misleading in assessing the applicability of different types of proppants, as the characterization of proppant-proppant and proppant-rock systems, at the grain-scale level, is in general overlooked in many practices.

Computational-based modeling including discrete element methods (DEM), or coupled discrete element method–computational fluid dynamics (DEM-CFD) have been proven to be handy tools in the study of complex processes such as hydraulic fracturing, fracture propagation and the performance of proppant-rock systems which controls production in unconventional reservoirs (Zeng and Zhang 2016, Zhang et al. 2017), while researchers have also used methods such as extended finite element method (FEM) or extended discontinuous deformation analysis in the study of complex problems involved in hydraulic fracturing. DEM-CFD modeling and other numerical tools which attempt to simulate discrete-based materials use contact laws as input (Coetzee 2017). These contact laws govern the interfaces of proppant-rock (and proppant-fluid-rock) systems. Therefore, investigation into the contact behavior and micromechanical-based modeling of proppants at their contacts is a crucial step in the study of complex processes involved in hydraulic fracturing. Micromechanical-based methods and microscopic considerations have also contributed in fields such as geothermal exploitation, the study of fractured rocks, ground-environment interaction, analysis of diagenetic processes or debris flow problems as well as jamming transition (e.g., Zhao and Shan 2013, Jiang et al. 2015, 2016, Jing et al. 2019, Song et al. 2020).

The permeabilities of fractured rocks in the presence of proppants are very important to be modeled at extremely small scales for accurate estimation of the production process (Zoback and Kohli 2019). This involves extremely small deformations of the rock and the proppant-rock systems which must be precisely modeled and their behavior may be governed, to an important extent, by the micro-scale morphological and compositional characteristics of the proppant and the rock (e.g., He and Senetakis 2020, Zoback and Kohli 2019, Zhang et al. 2020, Kasyap and Senetakis 2022). Thus, quantification of the deformations at the contacts of proppants, of the order of micrometers, is a crucial step encountered in hydraulic fracturing stimulation.

Experimental and theoretical studies into the contact problem of interfaces have provided important insights, with applications in various problems of engineering and science (e.g., Greenwood and Tripp 1971, Vu-Quoc et al. 2000, Mate 2008; Misra and Huang 2012, Medina et al. 2013, Zhai et al. 2016,

Chen et al. 2020). However, systematic experimental studies into the applicability of different contact mechanics models in natural sand grain systems de-coupling surface roughness and material type influences are very limited. Such studies would be instrumental in proppant modeling of natural quartz grains. Even though quartz sands have much smoother surfaces than many naturally occurring materials, they still have measurable roughness that may govern the interactions of proppants at the micro-level. For example, Sandeep et al. (2019) investigated the contact problem of two different natural materials including quartz sand grains (Ottawa sand) and a crushed basaltic rock, used as lunar simulant, and applied different normal and tangential contact models to investigate the constitutive behavior of the grains at their contacts. In that study, material type, hardness, meso-scale morphology and roughness were studied as coupled parameters. Yet, the study of grains of given composition and hardness, but with varying roughness, has not been examined systematically in the literature providing some valuable insights into the contact problem of proppants with implications in micromechanical-based simulations. Recently, Sandeep et al. (2021) investigated this problem (i.e., influence of roughness de-coupling that from the effect of material type), but their study focused on engineered grains composed of glass beads. Thus, there is a lot of scope in this field, particularly in the analysis of the behavior of natural sand grains used as proppant simulants.

In this study, three types of natural grains, which are considered as potential proppant simulants, are examined, which display relatively similar meso-scale morphologies and hardness, and the varying parameter is the surface roughness. Two contact models are applied: one considering roughness quantitatively, and the second one ignoring surface roughness. Outcomes from the study may contribute to the contact modeling of proppant interfaces. For example, in accurate modeling and prediction of the behavior of proppant-rock systems at the level of tens of nanometers to micrometers of displacement. Thus, outcomes from the study may contribute to future research using particulate-based discrete modeling in hydraulic fracturing problems. It is highlighted in the study that despite the relatively smooth surfaces of the natural quartz grains, their surface roughness is measurable enough to encounter significant plasticity at the early stages of deformations (i.e., the grains are still rough within a contact mechanics context), thus governing the proppant-proppant interactions which would not be expected for ideally perfectly smooth proppants.

2 Contact mechanics models

In this section, a brief review is presented on the two contact mechanics models used in the present study, which are used to simulate the normal contact behavior of the proppant simulants. These models will be later used to fit the experimental data to obtain contact parameters and also to check their reliability in imitating the force–displacement response of quartz sand particles.

2.1 Hertz contact model

Hertz (1882) proposed a non-linear elastic contact model for smooth non-conforming contacts. The Hertz model is widely used in the analysis of the normal loading behavior in various studies (for example, Teufelsbauer et al. 2009, Zhao et al. 2018, Li et al. 2021, Ren et al. 2021). When two grains of radius 'R'

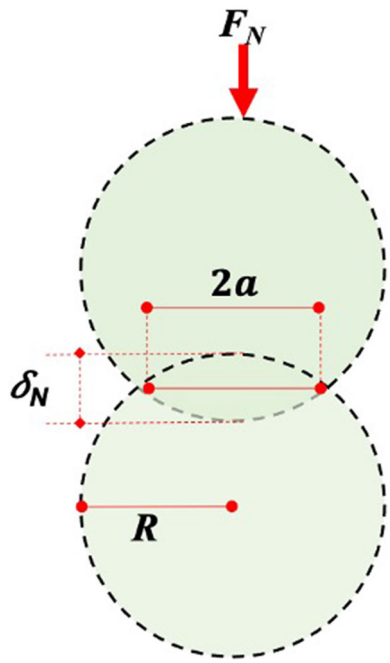

Fig. 1 Illustration of the normal loading of proppant-proppant contacts (considering perfect spheres in this example)

are subjected to a compressive force 'F_N' as shown in Fig. 1, it generates a circular contact area of radius 'a' which is calculated from Eq. (1) as follows:

$$a = \left(\frac{3RF_N}{8E^*}\right)^{\frac{1}{3}} \tag{1}$$

where E* is the equivalent Young's modulus of the two grains in contact, which is expressed as:

$$\frac{1}{E^*} = 2\left[\frac{1-\nu^2}{E}\right] \tag{2}$$

In Eq. (2), ν is the Poisson's ratio of the grains and the relationship between force and displacement (δ_N) is presented in Eq. (3):

$$F_N = \frac{2\sqrt{2}(R)^{\frac{1}{2}}E^*\delta_N^{\frac{3}{2}}}{3} \tag{3}$$

2.2 Yimsiri and Soga contact model

Yimsiri and Soga (2000) proposed an analytical model for rough grains in contact by considering an assembly of uniform-sized particles and the packing structure of the spheres was defined by incorporating a fabric tensor. Using micromechanical-based theory, they presented an association between force–displacement behavior at the grain scale and stress–strain behavior at the macroscopic level. They incorporated different contact laws, such as, the linear elastic, Hertz and rough surface contact models with some assumptions. The important assumptions were that no sliding occurs between the grains, the grains are not spinning and there is no resisting moment at the contacts. This model can be used to analyze the effects of contact characteristics, stress condition and fabric anisotropy on the small-strain behavior of granular materials.

Greenwood et al. (1984) and Johnson (1985) proposed a non-dimensional parameter (ω), expressed in Eq. (4), to study the variation of the asperity heights on the contact behavior:

$$\omega = 2\frac{S_q^*}{\delta_N} \tag{4}$$

where S_q^* is the equivalent surface roughness for two bodies in contact which follow an independent random distribution of asperities (not necessarily Gaussian) and it is presented in Eq. (5):

$$S_q^* = \sqrt{S_{q1}^2 + S_{q2}^2} \tag{5}$$

Yimsiri and Soga (2000) incorporated the surface roughness into their newly developed contact model through parameter ω. They showed that the radius ratio (a*/a) is a hyperbolic function of ω as presented in Eq. (6).

$$\frac{a^*}{a} = \frac{-2.8}{\omega + 2} + 2.4 \tag{6}$$

where a* is the circular contact radius of the rough grains.

Hertz model may be used as an approximation of very rough surfaces which display significant plastic deformations at the early stages of loading (Sandeep and Senetakis 2018a, b, Sandeep et al. 2019). Yimsiri and Soga model may be more applicable for very rough surfaces, but there are still some compromises in analyzing laboratory test data with this model (Sandeep et al. 2019, Ren et al. 2021).

3 Materials

Sandeep et al. (2018) carried out a micromechanical-based experimental study examining the tribological behavior of quartz sand grain contacts from different origins thus various morphological characteristics in terms of surface roughness. These sand grains can potentially be proppant simulants as they have relatively smoother surfaces than many other geological materials and their shapes are fairly regular. The aforementioned study focused on the frictional behavior of the grain interfaces with a limited discussion on their normal contact behavior. We recall the experimental data by Sandeep et al. (2018) and Sandeep 2019 to provide a detailed study into the compression behavior of the grains at their contacts, emphasizing the application of different contact mechanics models in order to fit the normal force–displacement curves. A previous discussion on the applicability of the Hertz model and also the Yimsiri and Soga model was presented by Sandeep et al. (2019) and Ren et al. (2021), but without de-coupling material type and surface morphology. For completeness, some of the characteristics of the materials are presented in this section. These soils are Leighton Buzzard sand (LBS), River sand (RS) and Beach sand (BS). LBS is a sand

from the UK which has been quarried from a location near to Bristol and has been widely studied and documented (Senetakis et al. 2013, Sandeep and Senetakis 2018a, b, Li et al. 2021). The River sand grains used in this study were obtained from Guangdong province, China. The Beach sand grains were obtained from the coastal region of Repulse Bay, Hong Kong. From visual observations, the grains of River sand and Beach sand are white to crystalline in color, while the LBS grains have yellow stains on their surfaces because of the presence of iron oxides.

The particle sizes of the grains used in this study were around 1–2 mm in average global diameter. These sizes may be a little larger than coarse proppants used in practice (e.g., Bandara et al. 2020a), but as mentioned by He and Senetakis (2020), these natural sand grains have such morphologies that their local radii (radii in the vicinity of the proppant-proppant and proppant-rock contacts) are much smaller compared with their global size. The local radius is what controls, predominantly, the contact behavior of natural grains as also pointed out by Sandeep and Senetakis (2018b), He and Senetakis (2019, 2020) and Sandeep (2019). Based on this, the local radii of the natural grains tested in the study may correspond to mesh 16/30–20/40, on average. The global radius would be expected to have less influence on the behavior of the proppants as the results by Sandeep (2019) would suggest.

The materials were observed under the Philips XL30 ESEM-FEG Environmental Scanning Electron Microscope (SEM) in order to obtain insights into their surface morphology and composition. This microscope is also equipped with EDS (Energy Dispersive X-ray Spectroscopy) to quantify the chemical composition in the samples. Figure 2 shows representative (SEM) images of the proppant simulants used in this study. These grains are sub-rounded to rounded in shape based on the Powers chart (after Powers 2009). All these grains are composed majorly of SiO_2 (more than 80%) with traces of other minerals and compounds.

The morphology of the proppants at the level of nano-to-micrometer was quantified in terms of the surface roughness. These measurements were taken on samples using an optical surface profiler (Veeco NT9300, after Sandeep et al. 2018). The vertical scanning interferometry (VSI) mode was applied for the scanning process, which allows for non-destructive assessment of the surface roughness. A field of view of 20 × 20 μm was used to scan the surface area, and the effect of curvature was removed to obtain the surface profiles. The roughness of the grains was quantified in terms of the root mean square (RMS) value denoted as S_q from Eq. (7):

$$S_q = \sqrt{\frac{1}{n}\sum_{i=1}^{n}\left(W_i^2\right)} \tag{7}$$

where n = the number of measured data points and W = the elevation relative to the base surface.

Figure 3 shows representative surface profiles of the proppant simulants used in this study. The average values of surface roughness for LBS, RS and BS based on ten measurements on each grain type were found to be 223 ± 51, 195 ± 30 and 293 ± 56 nm, respectively. The quartz sand grains chosen for this study are reasonably smooth compared with irregularly shaped and rough decomposed igneous and metamorphic rocks (Sandeep and Senetakis 2018a, c). Sandeep et al. (2018) observed that the surface roughness plays an essential role in the micromechanical behavior, particularly, affecting the inter-particle friction values. For example, the inter-particle coefficient of friction of LBS, RS and BS are 0.19 ± 0.04, 0.14 ± 0.02, 0.22 ± 0.06, respectively. The rougher BS grains have greater values of the inter-particle friction coefficient compared with RS and LBS. Detailed description regarding the tangential loading response of the quartz sands and the role of surface roughness were presented in Sandeep et al. (2018) and Sandeep (2019). It is noticed that despite the relatively low values of surfaces roughness as discussed above, the natural grains display morphological discrepancies as the coefficient of variation (defined as the ratio of standard deviation over the mean value of S_q) would range between 15 and 30% for the natural proppant simulants. These coefficients of variation are very similar with that of weathered rocks and crushed rock grains (e.g., Sandeep and Senetakis 2018a, c), so that these morphological discrepancies of natural grains, despite the overall low S_q values, cannot be ignored in assessing the contact behavior of proppant simulants and may contribute to scatter in the data in assessing their mechanical behavior. It is noted, however, that the coefficient of variation for the quartz sands of the present study is significantly lower compared with that

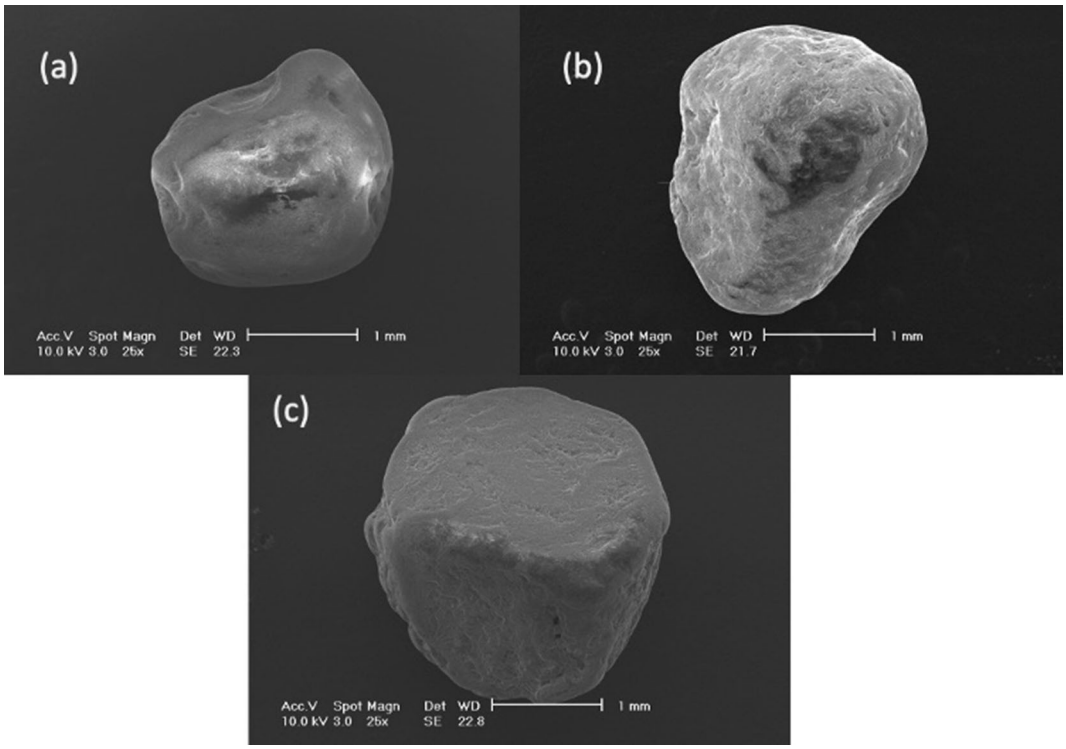

Fig. 2 Scanning electron microscope images of the three proppant simulants used in the study **a** LBS **b** River sand **c** Beach sand

of crushed limestone as reported by Senetakis et al. (2017).

4 Experimental setup

4.1 Sample construction

The experiments were performed using fairly regular in shape grains, which are handpicked for the micromechanical tests. The grains are glued to the cylindrical brass mounts ($\sim$8 mm in diameter) using Cyanoacrylate glue, a fast-acting adhesive. The specimen was then carefully pressed against the mount surface to reduce the quantity of glue between the grain and the mount. The works by Sandeep et al. (2018) and Sandeep (2019) showed that a period of 24 h is adequate for the hardening of the glue for these micromechanical tests.

4.2 Inter-particle loading apparatus

A micromechanical inter-particle loading apparatus (Fig. 4) housed at the City University of Hong Kong was used to simulate the proppant-proppant normal loading tests (technical descriptions may be found in more details in Sandeep et al. 2018). The apparatus is equipped with a stiff stainless-steel loading frame and three loading arms in three perpendicular directions. Each loading arm consists of a load cell (100 N capacity), a linear micro-stepper motor and an eddy current (non-contact) sensor, and the different electronic parts are rigidly connected with stiff mechanical components and linear bearings. The monitoring and controlling of the experiments are conducted with a dedicated software developed for the apparatus with a typical data recording of 0.33 Hz. The load cells have a precision of 0.02 N and the displacement sensors have a precision of 10^{-5} mm, so that the high accuracy measurements of forces and displacements allow for resolving contact stiffness which is particularly important to be quantified in accurate micromechanical-based modeling. The quality of the data is further improved using analog filters and high-quality amplifiers and data logging system. It is noticed that the City University of Hong Kong houses a range of grain-scale apparatus which are capable in the study of proppant-type and proppant-rock systems; these different setups

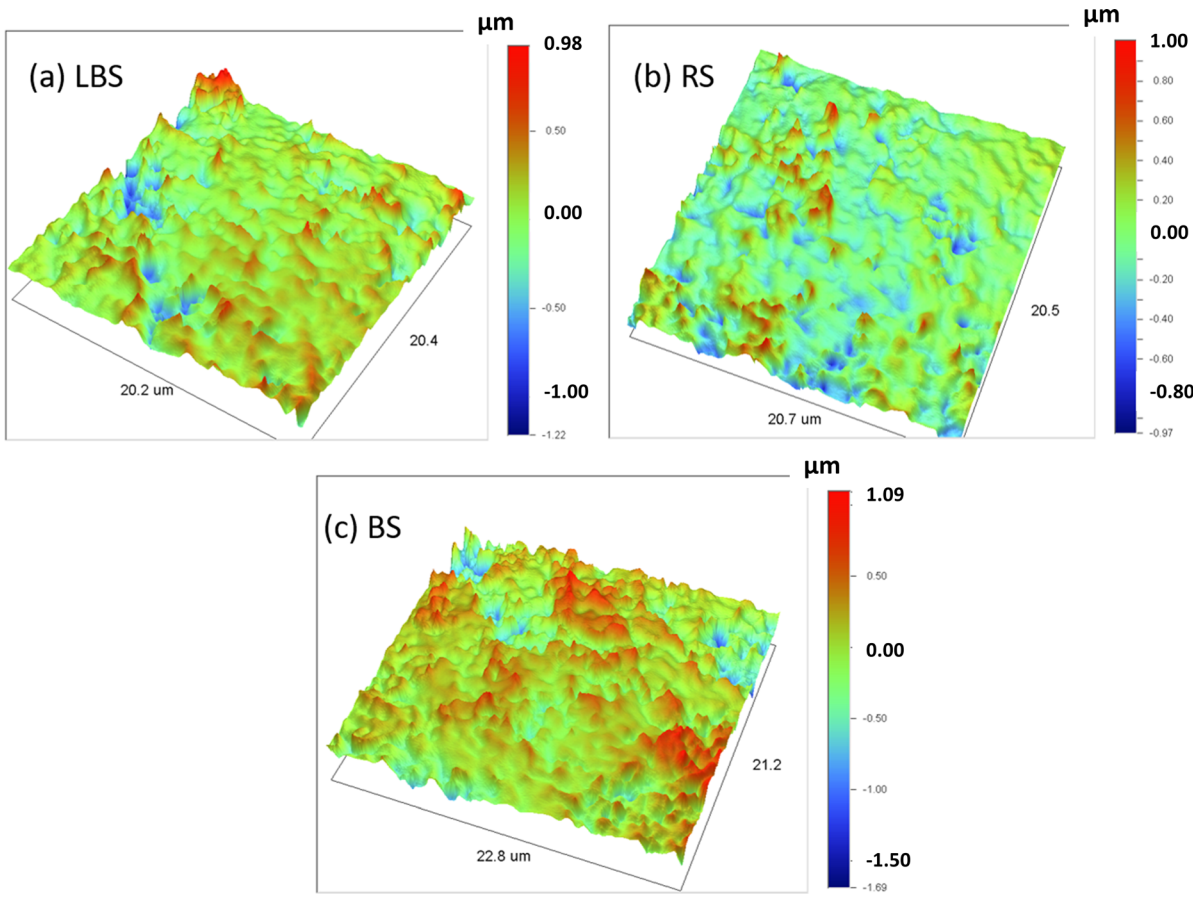

Fig. 3 Representative images from surface profiler analysis quantifying the roughness of the proppant simulants

have various capabilities in terms of loading rate and range of loads and displacements to be measured (and sample size as well). The apparatus used in the present study is more dedicated for smaller in size samples and for smaller in magnitude normal loads, so that emphasis in the present study, as will be discussed in subsequent sections, is placed on the transition from initially plastic behavior of asperities to a behavior with increased stiffness. However, all the experiments are performed well below the forces which would cause global damage to the grains. The global damage of grain contacts using LBS particles was recently investigated by Li et al. (2021), which study examined the influence of grain morphology on the interaction of pairs of grains close to the failure point.

After gluing the grains on the mounts and allowing them for 24 h for curing, the mounts were fixed on the top and bottom wells of the apparatus, which were then aligned in an apex-to-apex configuration through visual observations using digital micro-cameras from two orthogonal horizontal directions. The top well is connected to the vertical loading arm of the apparatus. The bottom well is fixed on a stainless-steel sled, which is connected to the horizontal loading arms. Note that one horizontal loading arm is typically used for the shearing and the second one is used to maintain the system in the out-of-plane direction. Based on an apex-to-apex configuration, the applied vertical force corresponds to the normal contact force to the specimen. Deviations from the verticality of the applied normal force can be detected and monitored, for example during the gradual application of the vertical force, which would give a reaction force to the horizontal loading systems (during the application of the vertical load, the two horizontally placed load cells are monitoring any lateral reactions of the system).

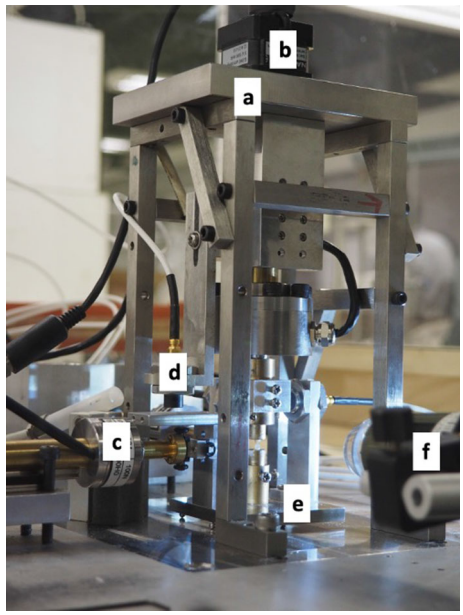

Fig. 4 Inter-particle loading apparatus at City University of Hong Kong used for the normal contact tests in the study **a** stainless steel loading frame **b** stepper motor **c** load cell **d** eddy current sensor **e** stainless steel sled **f** micro-camera

5 Results and discussions

5.1 Experimental observations

The high precision in the force and displacement measurements allows capturing the role of surface asperities on the normal loading behavior of the grains at their contacts. Figure 5a shows representative force–displacement curves for the proppant simulants during normal loading. It can be seen that, within the scatter on the data, the behavior is nearly similar for these three materials. The variabilities of the normal force–displacement curves are expected as these are natural sand grains and they have differences in their morphologies, both at the micro- and meso-scales resulting in a measurable coefficient of variation of S_q as mentioned earlier, as well as in discrepancies with respect to the local radius in the vicinity of the contacts which also influence the contact response (Sandeep et al. 2018, Sandeep and Senetakis 2018b, Li et al. 2021). The significance of meso-scale morphology would come into play more dominantly, especially for irregular-in-shape grains, but this would be expected to be more prevalent in the shearing direction and also in the analysis of the grain contact response close to

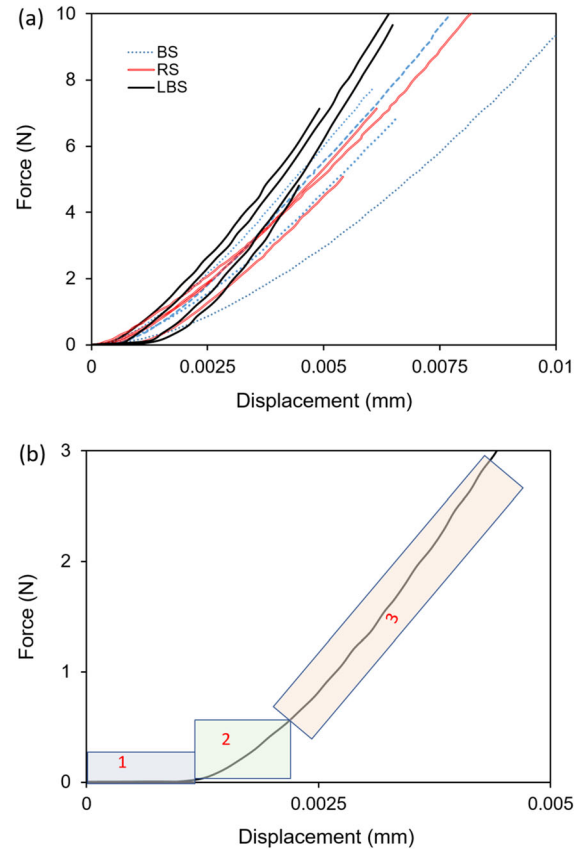

Fig. 5 **a** Force–displacement response of quartz sands (after Sandeep et al. 2018) **b** Different zones of response in a typical force–displacement curve corresponding to natural proppant simulants

the failure (crushing) of the particles (Li et al. 2021). A typical force–displacement response for geological materials can be categorized into three zones, as illustrated in Fig. 5b. The response is mainly controlled by the compression of surface asperities in zone 1 (deforming plastically); there is a transition in zone 2 (non-linear behavior) and a stiffer response in zone 3 (not necessarily Hertzian). In zone 3, a substantial increase in tangent stiffness is observed. This behavior (influence of roughness and distinct zones of behavior) has also been described in theoretical contact mechanics studies (Persson 2007, Pohrt and Popov 2012). According to the current study on quartz sand grains, the normal displacements in the zone 1 range from a few hundreds of nanometers up to approximately 1.5 µm. Previous studies on quartz sands (Sandeep and Senetakis 2018a, b, Sandeep et al. 2019) also observed a similar range of initial soft displacements

in zone 1. For much rougher grains (for example natural grains which have origin decomposed rocks or crushed rocks of very rough surfaces), zone 1 would be extended to 10 μm and beyond that point (Sandeep and Senetakis 2018a, Sandeep et al. 2019). For very smooth surfaces (e.g., almost perfectly smooth chrome steel balls), the initial regime of plastic displacements might be below 0.5 μm, or in some previous experiments performed at City University of Hong Kong, this initial regime would be almost absent for the lower bound of roughness values for chrome steel balls (Sandeep and Senetakis 2018a, Sandeep 2019).

Contact stiffness is an important input parameter in modeling the interactions of granular materials (and also fractured rock), but, in general, many numerical studies have ignored realistic values of contact stiffness in their analyses. The contact stiffness in the normal direction is obtained in the study by differentiating the forces against the displacements (using a sequence of 3–5 datapoints in the normal direction for the present experiments), deriving a tangent (or local) value of stiffness. Figure 6 shows normal stiffness-displacement curves for the quartz sands. The stiffness increased gradually with the displacement and this behavior is commonly observed for normal loading of rough surfaces. For very rough grains such as crushed basaltic rock used as lunar simulant (S_q = 1476 nm), Sandeep et al. (2019) also reported that the stiffness increased gradually with displacement. However, they observed very low values of normal stiffness (< 100 N/mm) for compression of the grain contacts up to 10 μm, whereas the present results demonstrate much higher normal stiffness for the quartz grains. According to the data in Fig. 6 (and also in Fig. 5a), the stiffness values for LBS and RS are at the upper end of the observed range for the three different types of proppant simulants, which is explained by the fact that these two types of grains have lower roughness values than BS.

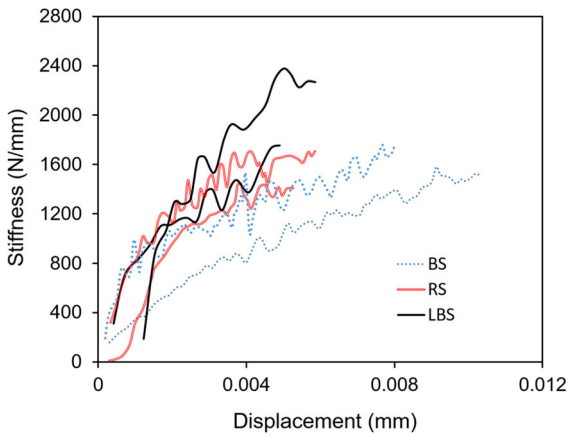

Fig. 6 Stiffness-displacement response for proppant simulants based on experimentally derived values

In many micromechanical-based numerical studies it is common to consider a constant ratio of tangential to normal stiffness (K_T/K_N), to be used as input in the study of granular systems and many times researchers consider $K_T/K_N = 1$. The stiffness-displacement curves of the proppant simulants show clearly that normal stiffness is a function of normal displacement with increasing K_N values as the compression at the grain contacts progresses. On the other hand, recalling data, for example by Sandeep et al. (2018, 2019), tangential stiffness (i.e., stiffness in the sliding direction) degrades very rapidly at the contacts of the grains (and subsequently at the contacts of the proppants). Additionally, recalling previous data on the tangential stiffness of the proppant simulants, the absolute values of normal contact stiffness and tangential stiffness are not so much related as the data would suggest, though both may have a dependency on material type and the morphology of the grains. Although the present study does not have a specific direction in investigating the relationship between K_T and K_N, these observations should be taken into consideration by researchers who simulate the hydraulic fracturing process with micromechanical-based discrete numerical tools.

5.2 Sensitivity of Yimsiri and Soga model

Yimsiri and Soga (2000) model incorporates, quantitatively, the effect of contact condition, in terms of roughness, between the grains in their model as shown in Eqs. (4–6). This can be particularly important in modeling the contact behavior of natural proppants which display measurable surface roughness (i.e. natural grains deviate from ideal perfectly smooth spheres). The sensitivity of this model in replicating the force–displacement behavior of quartz grain contacts is shown in Fig. 7. These plots correspond to "theoretically" produced curves from Yimsiri-Soga model using the input parameters as R = 1 mm, E = 100 GPa, ν = 0.1 for this illustrative example. The range of surface roughness values considered is between 150 and 350 nm, which is the typical range of

RMS roughness for quartz sand grains (Sandeep et al. 2018, Sandeep 2019).

From the visual observation of the curves in Fig. 7, it is seen that the normal load–displacement relationship is qualitatively similar to the trends observed for the natural quartz sand grains in the experiments (Fig. 5a). The model seems sensitive to the surface roughness and the initial soft response (Zone 1) as theoretically assessed, increases with increasing surface roughness. Additionally, there is a shift in the transition phase (zone 2); for example, with the change in surface roughness from 150 to 350 nm the range of zone 2 is shifted from 1.5–2.5 μm to 2.5–4.0 μm, respectively.

5.3 Modeling of experimental curves using Hertz and Yimsiri-Soga models

The experimental force–displacement curves were fitted using the models proposed by Hertz (1882) and Yimsiri and Soga (2000) and a representative case is shown in Fig. 8. The highlighted inset of the figure shows a closer view of the force–displacement response at smaller deformations. Figure 9 shows the stiffness-displacement response for the curves shown in Fig. 8. The solid black line corresponds to the experimental curve for the compression of two LBS grains and the dotted lines represent the theoretical (fitted) curves.

From the analysis presented in Fig. 8, it is observed that the Hertz model (dotted blue line) can reasonably simulate the force–displacement response of the proppant simulants after the regime of initial plastic

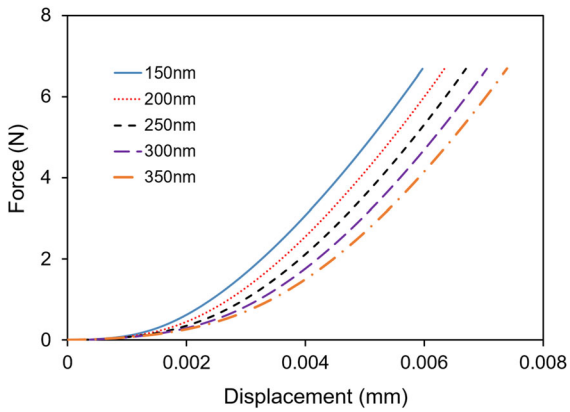

Fig. 7 Sensitivity of Yimsiri and Soga model to surface roughness: theoretical curves

displacements (1 μm). Similar behavior can also be seen in the stiffness-displacement curves (Fig. 9), where the Hertz model cannot simulate the response at smaller displacements, i.e., for displacements smaller than 2.5 μm for the given example. For fitting of the experimental curve in Figs. 8 and 9 using the Hertz model, a Young's modulus value of 53 GPa was used, which is much lower than the expected Young's modulus of the quartz (90–120 GPa, after Heyliger et al. 2003, Erdogan et al. 2017). As the Hertz model was developed, primarily, to simulate the response of ideally smooth surfaces, it is expected that this model cannot fit the initial regime where the asperities deform plastically, which is also observed in the force–displacement response of other geological materials (e.g., Sandeep et al. 2019, Ren et al. 2021). However, for grains with very low surface roughness values, such as steel balls (60 nm), the Young's modulus values obtained from Hertz fitting of the experimental curves are about 175 GPa (after Sandeep and Senetakis 2018a) which is very close to the expected Young's modulus value of the material (around 200 GPa based on material's specification). This suggests that the Hertz model performs better, on the point of view of deriving Young's modulus, for smoother and more regular in shape grains. However, it partly, does not capture the contact behavior of natural grains at very small displacements, which display morphologies which deviate from that of perfect smooth spheres.

In Figs. 8 and 9, the experimental data were also fitted with the rough surface contact model proposed by Yimsiri and Soga (2000). For the best fit of the model to the experimental data, a surface roughness value of 200 nm and a Young's modulus value of 150 GPa were used. These results suggest that the Yimisiri-Soga model can reasonably simulate the normal force–displacement and normal stiffness-displacement responses from the initial loading stages for natural quartz sand grains. This is attributed, predominantly, to the consideration of "reduced contact pressure" for rough surfaces through the inclusion of parameters a* and ω into the rough model. It is noted however that for the analysis, average values of RMS roughness were used for each material type into the expressions by Yimsiri-Soga, rather than the specific values of each given sample.

A comparison between the values of Young's moduli as derived from Hertz and Yimsiri-Soga

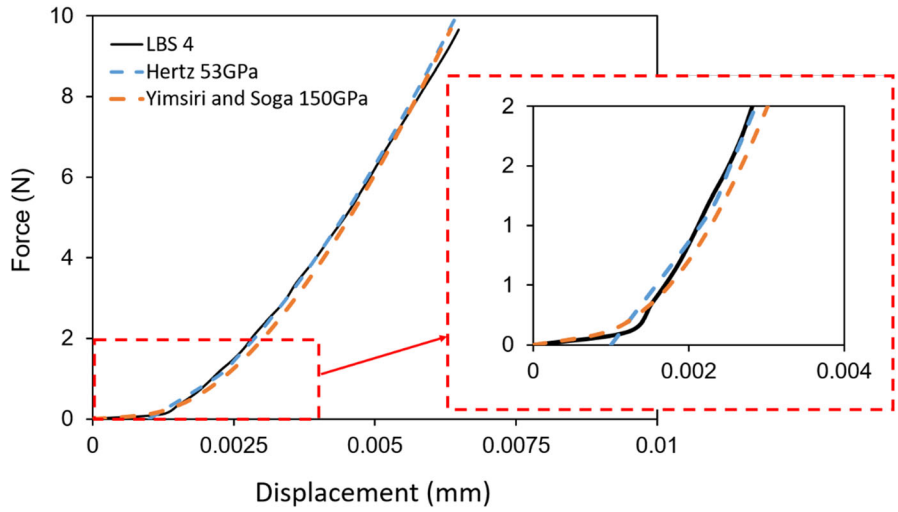

Fig. 8 Force–displacement response from experiment (black solid line) and contact models (dotted lines) based on best fit

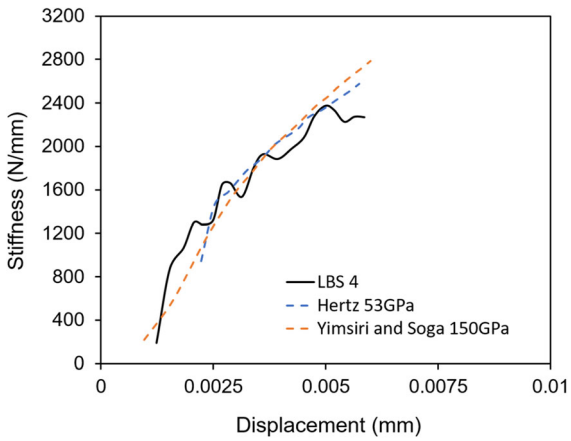

Fig. 9 Stiffness-displacement response from experiment (black solid line) and contact models (dotted lines) based on best fit

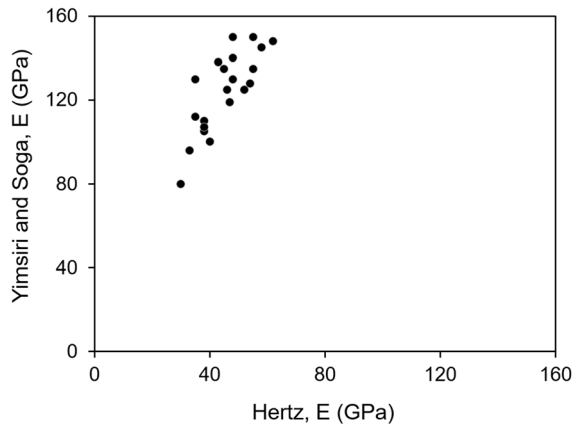

Fig. 10 Comparison between Young's modulus (E) values obtained from Yimsiri and Soga, and Hertz models for the proppant simulants: the rough model by Yimsiri and Soga provides significantly higher values of contact Young's modulus

models based on fitting to the experimental data for all the three proppant simulants included in the present study is given in Fig. 10. It is observed that the Young's modulus values from Hertz fitting are always lower than the excepted Young's modulus values and approximately 2–3 times lower than the values obtained using the Yimsiri-Soga model. The average values of Young's modulus from the fitting of these two models to the experimental curves are 45 ± 9 (Hertz) and 124 ± 19 GPa (Yimsiri-Soga), respectively, resulting in a slightly lower coefficient of variation for the rough surface model compared with the smooth surface model. For the quartz sands used in the present study with surface roughness ranging between 150–350 nm, the fitting using the Hertz model underestimated the Young's modulus by about 50–60%. In contrast, the Yimsiri-Soga model can satisfactorily fit the experimental data using material's Young's modulus (within a range of ±20%). It is recommended that user-defined models taking into account surface roughness parameters would be more desirable in discrete-based numerical simulations. The use of a rough model, such as Yimsiri-Soga expression, would have a better matching at the earlier stages of loading, where the deformations would be expected to be plastic for rough surfaces. However, the Hertz model, which is commonly adopted in many numerical analyses, can also be used. In this case, the Young's modulus should correspond to an apparent

value and not the real value of the mineral itself (i.e., Hertz model would incorporate roughness influence indirectly by taking a reduced material modulus). However, in this case a shift of the curve is desirable to capture the initial plastic deformations (i.e., at displacements in zone 1, the force should be zero or have values very close to zero displaying almost zero contact stiffness).

6 Conclusions

The normal contact behavior of rough quartz sand grains was investigated by applying fitting using two different normal contact models: (i) Hertz and (ii) Yimsiri and Soga. Based on their local radii the natural grains in the current study can be considered as proppant simulants and they would correspond to mesh 16/30–20/40, on average. The focus of the study was the investigation of the contact behavior of the proppants at very small deformations, as these deformations may be important to be considered in multi-scale problems where nano-to-micrometer scale of displacements are important to be encountered and modeled. The main conclusions are summarized as follows:

1. In the compression of rough grains, the force–displacement response is governed by the plastic deformation of surface asperities (zone 1) at the initial stages of loading, followed by a transition (zone 2) and finally a stiffer response (zone 3). The behavior in zone 2 is non-linear, while the behavior in zone 3 can be approximated by a linear relationship between normal force and normal displacement. Despite the application of small in magnitude normal forces, much below those that would induce global grain damage, because of the very small developed contact areas the stresses are high enough to trigger plasticity of the small asperities because of the very small contact area. This plasticity is dominant at the early stages of compression and is followed by a stiffer response.
2. For the range of surface roughness values of the three materials used in the study (150–350 nm), theoretical analysis of the Yimsiri-Soga rough surface model showed a relatively high sensitivity to changes in surface roughness and the displacement range of zones 1 and 2 was extended with increasing surface roughness, thus roughness governs the constitutive normal contact behavior on a theoretical standpoint.
3. The Hertz model could fairly simulate the proppant simulants' contact behavior only beyond zone 1 when a reduced Young's modulus value is used. For the rough quartz sand grains used in the current study, the Hertz model underestimated the Young's modulus by about 50–60%. Thus, the derived modulus corresponds in reality to an apparent value, but it is much closer to the real material modulus if the grains are very smooth and regular in shape. This observation may also imply that the application of different normal contact models may also depend on the proppant type in consideration as proppants may consist of ceramic (very smooth grains), or natural sand grains (with inherently rough surfaces).
4. The rough surface model had a better performance in fitting the normal contact force–displacement response of the natural proppant simulants from the initial stages of loading, where plasticity of asperities governs their behavior, while the fitted Young's modulus was very close to the expected value for quartz.
5. It is implied from the current experimental and analytical investigation that in using natural grains as proppants, even though their roughness is relatively low compared with many other naturally occurring materials, they are still rough enough to produce differences in the normal contact behavior which deviates from that of perfectly smooth spheres. In accurate modeling of hydraulic fracturing stimulation, such small deformation levels to be modeled, may impact the accuracy of theoretical studies so that considerations of the input contact models should be taken cautiously.
6. Normal contact stiffness increases with displacement. This has implications in discrete-based modeling as a key input parameter for estimating the ratio of tangential to normal contact stiffness (K_T/K_N). In the sliding direction, as theory and experiments presented in the literature suggest, tangential stiffness degrades rapidly as the sliding displacement increases so that the load (or stress) state of a contact in both the normal and tangential

directions is important to be assessed to assign appropriate (K_T/K_N) values.

7. The analysis from the proppant simulants would suggest that the use of a rough model in discrete-based analyses, such as Yimsiri-Soga expression, would have a better matching at the earlier stages of loading, where the deformations would be expected to be plastic for rough surfaces and additionally, real material modulus can be considered in this case. However, the Hertz model is directly implemented in many discrete-based numerical codes; in this case, the input modulus should correspond to a reduced value (or an apparent value) and not the real modulus of the material. This also implies that the Hertz model may incorporate, indirectly, roughness influence by taking a reduced material modulus compared with the real value of the material to be modeled. It is also recommended that in applying Hertz model, a shift of the curve is desirable to be considered to capture the initial plastic deformations. This again would depend on the roughness of the material as the increase in roughness in general shifts this zone of behavior to larger displacements.

Acknowledgements The work described in this article was fully supported by the grants from the Research Grants Council of the Hong Kong Special Administrative Region, China, Project No. "CityU 11210419" And Project No. "CityU 11214218".

Declarations

Conflict of interest The authors declare no conflict of interest with this submission.

References

Ahamed MAA, Perera MSA, Dong-yin Li, Ranjith PG, Matthai SK (2019) Proppant damage mechanisms in coal seam reservoirs during the hydraulic fracturing process: a review. Fuel 253:615–629

Bandara KMAS, Ranjith PG, Rathnaweera TD, Perera MSA, Kumari WGP (2018) Thermally-induced mechanical behaviour of a single proppant under compression: Insights into the long-term integrity of hydraulic fracturing in geothermal reservoirs. Measurement 120:76–91

Bandara KMAS, Ranjith PG, Rathnaweera TD, Wanniarachchi WAM, Yang SQ (2020) Crushing and embedment of proppant packs under cyclic loading: an insight to enhanced unconventional oil/gas recovery. Geosci Front. https://doi.org/10.1016/j.gsf.2020.02.017

Bandara KMAS, Ranjith PG, Rathnaweera TD (2020) Laboratory-scale study on proppant behaviour in unconventional oil and gas reservoir formations. J Nat Gas Sci Eng 78:103329

Chen X, Carpenter BM, Reches ZE (2020) Asperity failure control of stick-slip along brittle faults. Pure Appl Geophys. https://doi.org/10.1007/s00024-020-02434-y

Coetzee CJ (2017) Calibration of the discrete element method. Powder Technol 310:104–142

De Silva VRS, Ranjith PG (2019b) Evaluation of injection well patterns for optimum fracture network generation host-rock formations: an application in in-situ leaching. Miner Eng 2019(137):319–333

De Silva VRS, Ranjith PG (2019a) Intermittent and multi-stage fracture stimulation to optimise fracture propagation around a single injection well for enhanced in-situ leaching applications. Eng Fract Mech 220:106662

Dong KJC, He WH, Wang M (2019) Effect of surface wettability of ceramic proppant on oil flow performance in hydraulic fractures. Energy Sci Eng 7(2):504–514

Duan K, Kwok CY (2020) On the initiation, propagation and reorientation of simultaneously-induced multiple hydraulic fractures. Comput Geotech 117:103226

Erdogan ST, Forster AM, Stutzman PE, Garboczi EJ (2017) Particle-based characterization of Ottawa sand: Shape, size, mineralogy, and elastic moduli. Cement Concr Compos 83:36–44

Greenwood JA, Tripp JH (1971) The contact of two nominally flat rough surfaces. Proc Inst Mech Eng 185(1):625–633

Greenwood JA, Johnson KL, Matsubara E (1984) A surface roughness parameter in Hertz contact. Wear 100(1–3):47–57

He H, Senetakis K (2019) An experimental study on the micromechanical behavior of pumice. Acta Geotech 14(6):1883–1904

He H, Senetakis K (2020) A micromechanical study of shale rock-proppant composite interface. J Petrol Sci Eng 184:106542. https://doi.org/10.1016/j.petrol.2019.106542

He H, Luo L, Senetakis K (2020) Effect of normal load and shearing velocity on the interface friction of organic shale–proppant simulant. Tribol Int 144:106119. https://doi.org/10.1016/j.triboint.2019.106119

Hertz H (1882) Uber die Beruhrang fester elastischer Korper (On the contact of elastic solids). J Der Rennin Und Angew Math 92:156–171

Heyliger P, Ledbetter H, Kim S (2003) Elastic constants of natural quartz. J Acoust Soc Am 114(2):644–650

Jiang M, Shen Z, Wang J (2015) A novel three-dimensional contact model for granulates incorporating rolling and twisting resistances. Comput Geotech 65:147–163

Jiang M, Fu C, Cui L, Shen Z, Zhu F (2016) DEM simulations of methane hydrate exploitation by thermal recovery and depressurization methods. Comput Geotech 80:410–426

Jing L, Yang GC, Kwok CY, Sobral YD (2019) Flow regimes and dynamic similarity of immersed granular collapse: a CFD-DEM investigation. Powder Technol 345:532–543

Johnson KL (1985) Contact mechanics. Cambridge University Press, Cambridge

Kasyap SS, Senetakis K (2022) Characterization of two types of shale rocks from Guizhou China through micro-indentation, statistical and machine-learning tools. J Petrol Sci Eng 208:109304. https://doi.org/10.1016/j.petrol.2021.109304

Kwok CY, Duan K (2020) Modeling hydraulic fracturing in jointed shale formation with the use of fully-coupled discrete element method. Acta Geotech 15:245–264

Li S, Kasyap SS, Senetakis K (2021) A study on the failure behavior of sand grain contacts with Hertz modeling, image processing, and statistical analysis. Sensors 21:4611. https://doi.org/10.3390/s21134611

Mate CM (2008) Tribology on the small scale–a bottom up approach to friction, lubrication, and wear. Oxford University Press, Oxford (UK)

Medina S, Nowell D, Dini D (2013) Analytical and numerical models for tangential stiffness of rough elastic contacts. Tribol Lett 49(1):103–115

Misra A, Huang S (2012) Micromechanical stress–displacement model for rough interfaces: effect of asperity contact orientation on closure and shear behavior. Int J Solids Struct 49(1):111–120

Persson BNJ (2007) Relation between interfacial separation and load: a general theory of contact mechanics. Phys Rev Lett 99(12):125502

Pohrt R, Popov VL (2012) Normal contact stiffness of elastic solids with fractal rough surfaces. Phys Rev Lett 108(10):104301

Powers MC (2009) Comparison chart for estimating roundness and sphericity. The geoscience handbook (AGI data sheets), 8(4):167

Ren J, Li S, He H, Senetakis K (2021) The tribological behavior of iron tailing sand grain contacts in dry, water and biopolymer immersed states. Granul Matter 23(1):12. https://doi.org/10.1007/s10035-020-01068-0

Sandeep CS, Senetakis K (2018a) Effect of Young's modulus and surface roughness on the inter-particle friction of granular materials. Materials 11(2):217

Sandeep CS, Senetakis K (2018b) Grain-scale mechanics of quartz sand under normal and tangential loading. Tribol Int 117:261–271

Sandeep CS, Senetakis K (2018c) The tribological behavior of two potential-landslide saprolitic rocks. Pure Appl Geophys 175(12):4483–4499

Sandeep CS, He H, Senetakis K (2018) An experimental micromechanical study of sand grain contacts behavior from different geological environments. Eng Geol 246:176–186

Sandeep CS, Marzulli V, Cafaro F, Senetakis K, Pöschel T (2019) Micromechanical behavior of DNA-1A lunar regolith simulant in comparison to Ottawa sand. J Geophys Res Solid Earth 124(8):8077–8100. https://doi.org/10.1029/2019JB017589

Sandeep CS, Li S, Senetakis K (2021) Scale and surface morphology effects on the micromechanical contact behavior of granular materials. Tribol Int 159:106929. https://doi.org/10.1016/j.triboint.2021.106929

Sandeep CS (2019) Micromechanics of Hong Kong debris flow materials. PhD Thesis, in: architecture and civil engineering department, City University of Hong Kong

Senetakis K, Coop M, Todisco MC (2013) The inter-particle coefficient of friction at the contacts of Leighton Buzzard sand quartz minerals. Soils Found 53(5):746–755

Senetakis K, Sandeep CS, Todisco MC (2017) Dynamic inter-particle friction of crushed limestone surfaces. Tribol Int 111:1–8

Song Y, Ranjith PG, Wu B (2020) Development and experimental validation of a computational fluid dynamics-discrete element method sand production model. J Nat Gas Sci Eng 73:103052

Tang Y, Ranjith PG, Wu B (2019) Experimental study of effects of shearing on proppant embedment behaviour of tight gas sandstone reservoirs. J Pet Sci Eng 172:228–246

Teufelsbauer H, Wang Y, Chiou MC, Wu W (2009) Flow–obstacle interaction in rapid granular avalanches: DEM simulation and comparison with experiment. Granul Matter 11(4):209–220

Vu-Quoc L, Zhang X, Lesburg L (2000) A normal force-displacement model for contacting spheres accounting for plastic deformation: Force-driven formulation. J Appl Mech 76:363–371

Wang H, Sharma MM (2018) Modeling of hydraulic fracture closure on proppants with proppant settling. J Pet Sci Eng 171:636–645

Wang F, Li B, Chen Q, Zhang S (2019) Simulation of proppant distribution in hydraulically fractured shale network during shut-in periods. J Pet Sci Eng 178:467–474

Yang L, Wang D, Guo Y, Liu S (2016) Tribological behaviors of quartz sand particles for hydraulic fracturing. Tribol Int 102:485–496

Yimsiri S, Soga K (2000) Micromechanics-based stress–strain behaviour of soils at small strains. Geotechnique 50(5):559–571

Zeng J, Li H, Zhang D (2016) Numerical simulation of proppant transport in hydraulic fracture with the upscaling CFD-DEM method. J Nat Gas Sci Eng. https://doi.org/10.1016/j.jngse.2016.05.030

Zhai C, Gan Y, Hanaor D, Proust G, Retraint D (2016) The role of surface structure in normal contact stiffness. Exp Mech 56(3):359–368

Zhang F, Zhu H, Zhou H, Guo J, Huang B (2017) Discrete-element-method/computational-fluid-dynamics coupling simulaiton of proppant embedment and fracture conductivity after hydraulic fracturing. SPE. https://doi.org/10.2118/185172-PA

Zhang H, Liu S, Xiao H (2019a) Sliding friction of shale rock on dry quartz sand particles. Friction 7(4):307–315

Zhang H, Liu S, Xiao H (2019b) Tribological properties of sliding quartz sand particle and shale rock contact under water and guar gum aqueous solution in hydraulic fracturing. Tribol Int 129:416–426

Zhang CP, Cheng P, Ranjith PG, Lu YY, Zhou JP (2020) A comparative study of fracture surface roughness and flow characteristics between CO2 and water fracturing. J Nat Sci Eng 76:103188

Zhao J, Shan T (2013) Coupled CFD-DEM simulation of fluid–particle interaction in geomechanics. Powder Technol 239:248–258

Zhao S, Evans TM, Zhou X (2018) Effects of curvature-related DEM contact model on the macro-and micro-mechanical

behaviours of granular soils. Géotechnique 68(12):1085–1098

Zheng W, Tannant DD (2019) Influence of proppant fragmentation on fracture conductivity–insights from three-dimensional discrete element modeling. J Pet Sci Eng 177:1010–1023

Zoback MD, Kohli AH (2019) Unconventional reservoir geomechanics: shale gas, tight oil, and induced seismicity. Cambridge University Press